



HAL
open science

Kinetic and mechanistic study of the gas-phase reaction of ozone with γ -terpinene

Layal Fayad, Cécile Coeur, Thomas Fagniez, Nicolas Houzel, Gaël Mouret,
Xavier Sécordel

► **To cite this version:**

Layal Fayad, Cécile Coeur, Thomas Fagniez, Nicolas Houzel, Gaël Mouret, et al.. Kinetic and mechanistic study of the gas-phase reaction of ozone with γ -terpinene. *Atmospheric Environment*, 2021, 246, pp.118073. 10.1016/j.atmosenv.2020.118073 . hal-04290943

HAL Id: hal-04290943

<https://ulco.hal.science/hal-04290943>

Submitted on 22 Jul 2024

HAL is a multi-disciplinary open access archive for the deposit and dissemination of scientific research documents, whether they are published or not. The documents may come from teaching and research institutions in France or abroad, or from public or private research centers.

L'archive ouverte pluridisciplinaire **HAL**, est destinée au dépôt et à la diffusion de documents scientifiques de niveau recherche, publiés ou non, émanant des établissements d'enseignement et de recherche français ou étrangers, des laboratoires publics ou privés.



Distributed under a Creative Commons Attribution - NonCommercial 4.0 International License

1 **Kinetic and mechanistic study of the gas-phase reaction of ozone with γ -terpinene**

2

3 Layal FAYAD, Cécile COEUR*, Thomas FAGNIEZ, Xavier Secordel, Nicolas Houzel and

4 Gaël MOURET

5

6 Laboratoire de Physico-Chimie de l'Atmosphère, Université du Littoral Côte d'Opale, 189A

7 Avenue Maurice Schumann, Dunkerque, France

8

9 *Corresponding author. Tel.: +33 328 23 76 42

10 Email address: coeur@univ-littoral.fr (C. Coeur).

11

12

13 **Abstract**

14 The ozone reaction of γ -terpinene (1-isopropyl-4-methyl-1,4-cyclohexadiene), a
15 monoterpe emitted by Elm, Cypress, Waterhickory and Maple trees, has been investigated
16 at 294 ± 2 K, atmospheric pressure and under dry conditions (relative humidity, RH < 2 %) in
17 two simulation chambers of the LPCA laboratory in Dunkerque (France): CHARME
18 (CHamber for the Atmospheric Reactivity and the Metrology of the Environment) a 9.2 m^3
19 evacuable cylinder in stainless steel electropolished and LPCA-ONE a 8 m^3 cubic reactor in
20 PMMA. Cyclohexane was used to scavenge the hydroxyl radicals formed from the
21 rearrangement of the Criegee biradicals. The concentrations of the organic compounds were
22 monitored versus the time with a PTR-ToF-MS and a TD-GC-FID. The rate coefficient for
23 the γ -terpinene reaction with ozone has been determined using the pseudo first-order and the
24 relative-rate methods. The values obtained with both methods are in a very good agreement
25 and give an average value of $(2.10 \pm 0.11) \times 10^{-16} \text{ cm}^3 \text{ molecule}^{-1} \text{ s}^{-1}$ which leads to an
26 atmospheric lifetime of 32 minutes for γ -terpinene with respect to its ozonolysis reaction. The

27 main oxidation products observed and their respective molar yields (in %) include formic acid
28 (7 - 11), glyoxal and/or acetone (4 - 9), 3-oxobutanal (6 - 8), 4-methyl-3-oxopentanal (5 - 8),
29 acetic acid (5 - 9), acetaldehyde (3 - 6), formaldehyde (3 - 6), 3-oxopropanoic acid (2 - 4) and
30 an unidentified compound with m/z 73.0 (2 - 3). The kinetic data are compared with the
31 literature, and the reaction mechanism is discussed. To our knowledge this work represents
32 the first mechanistic study for the ozonolysis reaction of γ -terpinene.

33

34 **Keywords:** simulation chamber, γ -terpinene ozonolysis, rate coefficient, mechanistic study.

35

36

37 **1. Introduction**

38 Volatile Organic Compounds (VOCs) are emitted into the atmosphere from both natural and
39 anthropogenic sources. On a global scale, the emissions of natural VOCs exceed
40 anthropogenic ones by a factor of about 10 (Lamb et al., 1987; Guenther et al., 1995).
41 Biogenic volatile organic compounds (BVOCs) are mainly emitted from vegetation (Guenther
42 et al., 1995), and they consist of isoprene (44 %) and monoterpenes (11 %). The emission
43 fluxes of these BVOCs depend on the cover and type of vegetation, temperature, irradiation,
44 ambient concentration of carbon dioxide and soil humidity (Peñuelas and Staudt, 2010).
45 BVOCs are key compounds for the physical and chemical properties of the atmosphere and
46 climate (Calfapietra et al., 2013). They influence the oxidative capacity of the atmosphere and
47 impact the tropospheric ozone budget. They also contribute to the formation of secondary
48 organic aerosols (SOAs), and hence affect the gas phase and the heterogeneous chemistry of
49 the troposphere (Hoffmann et al., 1997; Mackenzie-Rae et al., 2017a). BVOCs are oxidized in
50 the atmosphere and these atmospheric degradation processes are initiated in the gas phase by
51 the attack of hydroxyl radical during daytime and by nitrate radicals during the night

52 (Finlayson-Pitts and Pitts Jr, 1999). BVOCs also react with ozone, during both night and day
53 and the ozonolysis reactions of these unsaturated compounds are known to represent a
54 significant source of OH radicals (Johnson and Marston, 2008). Among the different classes
55 of BVOCs, monoterpenes ($C_{10}H_{16}$), whose structures are built up from two isoprene (C_5H_8)
56 units, are considered to be of great importance in the atmosphere. They are very reactive and
57 their atmospheric chemical lifetime ranges from minutes to hours. The most abundant
58 monoterpenes are α -pinene and β -pinene (Guenther et al., 1995). γ -terpinene (1-isopropyl-4-
59 methyl-1,4-cyclohexadiene) is a monoterpene emitted into the atmosphere from Elm, Cypress,
60 Waterhickory and Maple trees (Khalil and Rasmussen, 1992; Rasmussen, 2012); its volumes
61 ratios in the atmosphere are about a few pptv (Bouvier-Brown et al., 2009).

62 It is identified as an antioxidant in various essential oils like cumin oil and is used in
63 fragrances and flavors. The presence of two endocyclic C=C double bonds makes γ -terpinene
64 a reactive VOC and gives it the possibility to be oxidized into various products in the gas
65 phase.

66 Previous works on the ozonolysis reaction of γ -terpinene have been performed. Grimsrud, et
67 al. (1974) and Atkinson et al. (1990) have determined the rate coefficient using the absolute
68 and relative-rate method, respectively, however the values they obtained disagree with a
69 relative discrepancy of $\approx 50\%$.

70 The aim of this work was to study in a simulation chamber the atmospheric reactivity of γ -
71 terpinene with ozone. The rate coefficient was determined using the pseudo-first-order and the
72 relative-rate methods and the obtained value was compared with literature data. In addition,
73 the oxidation products formed in the gas phase were characterized and quantified and the
74 mechanism leading to the main degradation products is proposed. To our knowledge this
75 work represents the first mechanistic study for the ozonolysis reaction of γ -terpinene in the
76 atmosphere.

77

78 **2. Material and methods**

79 The experiments were performed in the dark, at $294 \pm 2\text{K}$, atmospheric pressure, and dry
80 conditions ($\text{RH} < 2\%$) in two atmospheric simulation reactors: CHARME (CHamber for the
81 Atmospheric Reactivity and the Metrology of the Environment) and LPCA-ONE. CHARME
82 is a new reaction chamber designed in the LPCA (Laboratoire de Physico-Chimie de
83 l'Atmosphere) laboratory in Dunkerque (France). It is a 9.2 m^3 (length of $\approx 4\text{ m}$, diameter of
84 $\approx 1.7\text{ m}$ and surface to volume ratio of $\approx 3.5\text{ m}^{-1}$) evacuable cylinder in electro-polished
85 stainless steel (304 L). Four stainless steel fans positioned at the bottom of the chamber allow
86 the homogenization of the gaseous mixtures. The temperature and relative humidity were
87 controlled using a combined T / RH probe (HMT334 series transmitters, VAISALA). The
88 CHARME chamber was pumped down to 0.4 mbar with a vacuum pump (Cobra NC0100-
89 0300B) and was then filled till the atmospheric pressure with purified and dried air using a
90 generator (Parker Zander KA-MT 1-8). The LPCA-ONE chamber is described in detail in
91 Lauraguais et al. (2012). Briefly, it consists of a 8 m^3 cubic reactor in PPMA (PolyMethyl
92 Methacrylate) equipped with a fan to ensure homogeneous mixing of the reactants. Prior to
93 each experiment, the reaction chamber was flushed with purified air for about 12 h (air
94 generator; Dominick Hunter LGCAD 140). The ozonolysis reactions were performed in the
95 presence of an excess of cyclohexane to scavenge the hydroxyl radicals produced from the
96 rearrangement of the Criegee biradicals (Henry and Donahue, 2011). The cyclohexane
97 concentrations were calculated in order to scavenge more than 95% of the OH radicals formed
98 (i.e. $k_{(\text{cyclohexane}+\text{OH})} \times [\text{cyclohexane}] / k_{(\gamma\text{-terpinene}+\text{OH})} \times [\gamma\text{-terpinene}] \geq 10$).

99 In CHARME, the organic compounds were first injected into the chamber using a glass
100 impinger and their concentrations were continuously recorded using a proton transfer reaction
101 time of flight mass spectrometer (PTR-ToF-MS 1000, IONICON Analytik, Innsbruck,

102 Austria). The PTR-ToF-MS allows the detection of any chemical compounds that have a
103 proton affinity higher than that of water. It uses hydronium ions (H_3O^+) to chemically ionize
104 compounds through a proton transfer reaction and then identify them by their mass to charge
105 ratio (m/z). The detailed principle of operation for the PTR is mentioned in Blake et al.,
106 (2009). The analytes were sampled by an inlet PEEK capillary line of 100 cm heated at 333 K
107 to reduce the loss of the VOCs during their sampling and then ionized in the drift tube ($E =$
108 $600 \text{ V}\cdot\text{cm}^{-1}$; $E/N=136 \text{ Td}$) which operates at 2.2 mbar and 333 K. To monitor the reactant
109 concentrations, the ion at m/z 137.2, corresponding to its parent $[\text{M}+\text{H}]^+$ ion, was recorded for
110 γ -terpinene and the one at 71.1 for the reference compounds, *cis*-2-pentene and 2-methyl-2-
111 butene (both compounds have the same molecular formula, C_5H_{10}). In the PTR-ToF-MS, γ -
112 terpinene is fragmented in two peaks at m/z 81.0 ($\approx 65\%$) and m/z 137.2 ($\approx 35\%$). As the main
113 peak interferes with some products formed during the ozonolysis reaction, it was not selected
114 to follow the γ -terpinene concentrations.

115 In LPCA-ONE, known volumes of VOCs were injected through a heated injector, sampled on
116 stainless steel tubes filled with Tenax TA (60-80 mesh) and then thermodesorbed and
117 analyzed with a ThermoDesorber - Gas Chromatograph - Flame Ionization Detector (TD-GC-
118 FID; Autosystem XL, Perkin Elmer). The organics were separated onto a 30 m DB-5 capillary
119 column held at 353 K during 5 min and then programmed to 523 at 5 K min^{-1} . Due to
120 overlapping peak with γ -terpinene at m/z 137.2 in the PTR-ToF-MS, the TD-GC-FID method
121 was used for kinetic studies using α -pinene as reference compound.

122 Preliminary tests were performed for each organic compound to control the linearity of the
123 PTR-MS and the GC-FID with respect to the injected VOC concentrations and also to verify
124 the absence of interferences between γ -terpinene or the references and their oxidation
125 products. The wall losses of organic compounds were also investigated in both chambers.
126 They were determined in the dark from the decay of their concentrations before the ozone

127 introduction and were considered as negligible for γ -terpinene, α -pinene, cis-2-pentene and 2-
128 methyl-2-butene (for these 4 VOCs, $k_{\text{wall loss}} = (7 - 9) \times 10^{-6} \text{ s}^{-1}$). Ozone was introduced into
129 the chambers using an ozone generator (Air Tree Ozone Technology C-L010-DTI) that
130 converts pure oxygen to ozone with a high voltage corona discharge and its concentrations
131 were monitored by an UV photometric ozone analyzer (Thermo Scientific 49i). The initial
132 mixing ratios used ranged from 43 to 800 ppbv for organic compounds and from 200 to 5300
133 ppbv for ozone. Acetonitrile (2.5 μL) was injected in all the experiments as a dilution tracer.
134 Oxidation products were analyzed in the gas-phase with the PTR-ToF-MS. For formaldehyde
135 ($m/z = 31.0$), formic acid ($m/z = 47.0$), acetone ($m/z = 59.0$), acetic acid ($m/z = 61.0$) and γ -
136 terpinene ($m/z = 137.2$) the instrument was calibrated from injection of known volumes of
137 standards into the chamber. However, for most of the oxidation products, the volume ratios
138 were determined using a generic H_3O^+ rate coefficient for their protonation reaction of 2×10^9
139 $\text{cm}^3 \text{ molecule}^{-1} \text{ s}^{-1}$. Certain compounds are subject to fragmentation. This is the case for
140 example for glyoxal which fragments into an ion at m/z 31 (Stonner et al., 2017) and then
141 interferes with the formaldehyde parent ion and for acetic acid (Haase et al. (2012);
142 Baasandori et al. (2015)). So, the uncertainties on the determination of the concentrations of
143 VOCs having low masses can be important and it has been estimated that the uncertainties on
144 the formation yields of these oxidation products are around 50 %.

145 The compounds used in this work, their manufacturer, and stated purity were as follows: γ -
146 terpinene (ACROS ORGANICS, 97%), α -pinene (ACROS ORGANICS, 98.0%),
147 cyclohexane (CHEM-LAB, $\geq 99.5\%$), cis-2-pentene (SIGMA-ALDRICH, 98.0%), 2-methyl-
148 2-butene (SIGMA-ALDRICH $> 99.0\%$), acetone (VERBIESE, 99.5%), acetonitrile (SIGMA-
149 ALDRICH, $\geq 99.5\%$), acetic acid (SIGMA-ALDRICH $\geq 99.5\%$), formic acid (Fisher
150 Scientific, 98%), formaldehyde (J.T.Baker, 37% stabilized with methanol 10-15%), and

151 oxygen (PRAXAIR 99.9999%). Pure dry air was supplied by a compressed air adsorption
152 dryer Zander KA-MT 1-8 (Parker).

153

154 **3. Results and Discussion**

155 **3.1. Rate constant determination**

156 The rate constant for the reaction of γ -terpinene and ozone was determined through two
157 different kinetic methods, the pseudo-first-order and the relative-rate method.

158

159 **3.1.1. Pseudo-first-order kinetics**

160 A set of eleven experiments was performed under pseudo-first-order conditions with an
161 excess of ozone. The initial concentrations ranged from 43 to 497 ppbv for γ -terpinene and
162 from 450 to 5300 ppbv for ozone. To ensure that pseudo-first-order conditions prevailed, the
163 initial ozone concentrations were at least ten times higher than those of γ -terpinene.

164

165 The γ -terpinene decay due to its reaction with O_3 is described as followed:

166



168 $-\frac{d[\gamma\text{-terpinene}]}{dt} = k_{\gamma\text{-t}} \times [O_3] \times [\gamma\text{-terpinene}]$ (I)

169 By replacing $k_{\gamma\text{-t}} \times [O_3]$ by the pseudo-first-order rate coefficient $k'_{\gamma\text{-t}}$ (in s^{-1}), equation (I) can be
170 simplified into:

171 $-\frac{d[\gamma\text{-terpinene}]}{dt} = k'_{\gamma\text{-t}} \times [\gamma\text{-terpinene}]$ (II)

172 The integration of equation (II) leads to the following relationship:

173 $\frac{\ln[\gamma\text{-terpinene}]_0}{\ln[\gamma\text{-terpinene}]_t} = k'_{\gamma\text{-t}} \times t$ (III)

174 where $k_{\gamma t}$ is the rate coefficient for the reaction of γ -terpinene with ozone (reaction 1), and the
175 subscripts 0 and t indicate concentrations at the start of the reaction and at a time t ,
176 respectively.

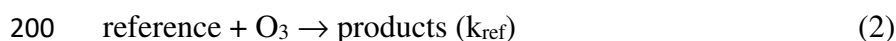
177 The rate coefficient $k'_{\gamma t}$ are deduced from the straight lines of the plots of $\ln([\gamma\text{-terpinene}]_0/[\gamma\text{-}$
178 $\text{terpinene}]_t)$ versus the time according to equation (III) (see Fig. S1. Supporting Information).

179 The uncertainties on the measurement of $k'_{\gamma t}$ are twice the standard deviation arising from the
180 linear regression analyses of the slopes of $\ln([\gamma\text{-terpinene}]_0/[\gamma\text{-terpinene}]_t)$ as a function of
181 time; they are in the range 0.02-0.04%. $k_{\gamma t}$ is determined from the plot of the obtained $k'_{\gamma t}$
182 values versus the initial ozone concentrations as shown in Fig. 1. Indicated error on the
183 measurement of $k_{\gamma t}$ include both the relative uncertainties on the determination of $k'_{\gamma t}$ and
184 that on the measurement of the O_3 concentration (relative uncertainty = 5%). The rate
185 coefficient determined using this method is $k_{\gamma t} = (2.03 \pm 0.10) \times 10^{-16} \text{ cm}^3 \text{ molecule s}^{-1}$ (see
186 table 1). The indicated errors (in the range 0.03-0.07 %) are twice the standard deviation
187 arising from the linear regression analysis of the data.

188

189 **3.1.2. Relative-Rate Method**

190 The rate constant of the ozonolysis of γ -terpinene was also obtained with the relative-rate
191 kinetic method. Three references compounds were used and a minimum of three experiments
192 were performed for each of them. The references used in this study and their rate coefficients
193 with ozone (in units of $\text{cm}^3 \text{ molecule}^{-1} \text{ s}^{-1}$) were 2-methyl-2-butene ($k_{(2\text{-methyl-2-butene})} = (4.1 \pm$
194 $0.5) \times 10^{-16}$; Witter et al., 2002), cis-2-pentene ($k_{(\text{cis-2-pentene})} = (1.32 \pm 0.04) \times 10^{-16}$;
195 Avzianova and Ariya, 2002) and α -pinene ($k_{(\alpha\text{-pinene})} = (9.6 \pm 0.15) \times 10^{-16}$; IUPAC current
196 recommendation). These experiments were performed with an OH scavenger (cyclohexane).
197 The rate coefficient with ozone was determined by comparing the decay rate of γ -terpinene
198 relative to that of the references.



201

202 Kinetic treatment of reactions 1-2 leads to the following relationship:

203
$$\ln \frac{[\gamma\text{-terpinene}]_0}{[\gamma\text{-terpinene}]_t} = \frac{k_{\gamma-t}}{k_{ref}} \times \ln \frac{[\text{reference}]_0}{[\text{reference}]_t} \quad (\text{IV})$$

204 where $k_{\gamma-t}$ and k_{ref} are the rate coefficients for the reactions of γ -terpinene and the references
205 with ozone (reactions 1 and 2), respectively, and the subscripts 0 and t indicate concentrations
206 at the start of the reaction and at a time t , respectively.

207 The VOC concentrations measured versus the reaction time were plotted in the form of
208 equation IV and the obtained plots show a good linearity with near zero intercept (Fig. 2). The
209 slopes ($k_{\gamma-t}/k_{ref}$) derived from the plots and the calculated ozone rate coefficients ($k_{\gamma-t}$) are
210 displayed in table 1. The indicated errors are twice the standard deviations arising from the
211 least squares linear regression of the data and do not include the uncertainties in the reference
212 rate coefficients.

213

214 Rather than calculating an average rate coefficient for the γ -terpinene using the different
215 reference compounds, a more representative values for $k_{\gamma-t}$ was obtained by combining the
216 data recorded for the three references into one plot represented by eq V. This plot is also
217 linear with near-zero intercept (see Fig. S2. Supporting Information).

218
$$k_{ref} \times \ln \frac{[\gamma\text{-terpinene}]_0}{[\gamma\text{-terpinene}]_t} = k_{\gamma-t} \times \ln \frac{[\text{reference}]_0}{[\text{reference}]_t} \quad (\text{V})$$

219

220 The rate coefficients for the reaction of γ -terpinene with ozone determined with the relative-
221 rate method using the three references are in accordance (relative discrepancy lower than 5 %) and
222 lead to an average value of $k_{(\gamma\text{-terpinene})} = (2.17 \pm 0.11) \times 10^{-16} \text{ cm}^3 \text{ molecule}^{-1} \text{ s}^{-1}$. This

223 value is also in good agreement with the rate coefficient measured with the pseudo-first-order
224 method ($k_{(\gamma\text{-terpinene})} = (2.03 \pm 0.10) \times 10^{-16} \text{ cm}^3 \text{ molecule s}^{-1}$), so this provides a good
225 confidence in the data determined in the present work for the γ -terpinene reaction with ozone.
226 So, based on these two methods, the mean rate coefficients for the reaction of γ -terpinene with
227 ozone is $k_{(\gamma\text{-terpinene})} = (2.10 \pm 0.11) \times 10^{-16} \text{ cm}^3 \text{ molecule s}^{-1}$. Indicated errors are twice the
228 standard deviation arising from the linear regression analysis and do not include the
229 uncertainty in the reference rate coefficients. This rate coefficient can be compared with
230 literature data as well. Two previous determinations were reported as it is shown in table 1.
231 The rate coefficient obtained by Atkinson et al. (1990) using the relative-rate method ($k_{(\gamma\text{-}$
232 $\text{terpinene})} = (1.63 \pm 0.12) \times 10^{-16} \text{ cm}^3 \text{ molecule s}^{-1}$; this value has been recalculated using the
233 current recommended value for the reference compound, α -pinene (IUPAC)) is $\approx 22 \%$ lower
234 than the one obtained in the present work. As this difference is within an acceptable 20-25%
235 error margin, both values can be considered to be in accordance. On the contrary, the rate
236 coefficient reported by Grimsrud et al. (1974) with the absolute method ($k_{(\gamma\text{-terpinene})} = 2.84 \times$
237 $10^{-16} \text{ cm}^3 \text{ molecule s}^{-1}$) is $\approx 39 \%$ higher and does not match with that determined in this
238 study. In their study, Atkinson et al., (1990) determined consistently lower rate coefficients
239 (from a factor of ≈ 2 to 6) for monoterpenes (e.g. β -pinene, α -pinene, α -phellandrene and γ -
240 terpinene) than Grimsrud, et al. (1974). Atkinson et al., (1990) suggested that the highest
241 values reported by Grimsrud, et al., (1974) were probably due to secondary reactions which
242 occurred at atmospheric pressure in the slow flow system used to perform the experiments.

243

244 **2. Gas-phase oxidation products**

245 A total of five experiments were carried out in the dark using the CHARME chamber to
246 characterize the products formed from the gas phase from the oxidation of γ -terpinene with
247 ozone. PTR-ToF-MS analyses were continuously performed during the ozonolysis reaction to

248 monitor the concentration of the organics versus the time. The peaks which were detected
249 along the course of the experiments are listed in table 2 and their typical time profiles are
250 displayed in Fig. 3. The concentrations have been corrected for their backgrounds signals
251 recorded before the ozone introduction.

252
253 γ -terpinene was first introduced into the chamber and followed throughout the experiment
254 with the PTR-ToF-MS at m/z 137.2. Cyclohexane was then injected and theoretically as its
255 proton affinity is lower than that of water, it should not be detected by the PTR-ToF-MS.
256 However, a peak at m/z 85.1 was observed during/after its introduction, suggesting that it
257 likely corresponds to cyclohexane. This peak was also detected by Lee et al., (2006) and
258 Mackenzie-Rae et al. (2017) in similar investigations, and seems to result from termolecular
259 reactions in the PTR-ToF-MS (Smith and Španěl, 2005). Acetonitrile was injected as a
260 dilution tracer and followed throughout the experiment at m/z 42.0. Its signal remained
261 constant indicating that dilution effects in the chamber are negligible.

262 As soon as ozone is introduced, γ -terpinene is rapidly oxidized (within a few minutes) to form
263 a number of oxidation products whose concentrations continuously increase during the
264 experiment and then reach a plateau when the γ -terpinene is totally consumed. Meanwhile, the
265 ozone concentration displays a rapid initial consumption followed by a slow decrease in part
266 due to wall losses ($k_{\text{wall}(\text{O}_3)} \approx 3 \times 10^{-5} \text{ s}^{-1}$).

267 18 compounds were observed with the PTR-ToF-MS (see table 2 and Fig. 3) and 12 of them
268 were identified using their m/z ratio as well as the proposed chemical mechanism (Fig. 6)
269 leading to these chemical species.

270 For the 9 most abundant oxidation products, the formation yields were determined from the
271 plot of their concentrations versus the amount of γ -terpinene consumed (Fig. 4). The yields
272 obtained from the slope of the linear least-squares fit to the data are also shown in table 2.

273 The major oxidation products observed and their respective molar yields are (the indicated
274 m/z include the addition of H⁺): formic acid (m/z 47.0; 7 - 11 %), glyoxal and/or acetone (m/z
275 59.0; 4 - 9 %), 3-oxobutanal (m/z 87.0 ; 6 – 8%), 4-methyl-3-oxopentanal (m/z 115.1; 5 - 8
276 %), acetic acid (m/z 61.0; 5 - 9 %), acetaldehyde (m/z 45.0; 3 - 6 %), formaldehyde (m/z 31.0;
277 3 - 6 %), 3-oxopropanoic acid (m/z 89.0 ; 2 - 4) and an unidentified compound (m/z 73.0; 2 -
278 3 %).

279 9 minor compounds were also formed from the gas-phase reaction of ozone with γ -terpinene:
280 2-oxosuccinaldehyde (m/z 101.0; < 1%); γ -terpinonaldehyde (m/z 169.2; < 1%);
281 C₄H₆O₃H⁺(m/z 103.1 ; 1 - 2 %); C₆H₁₀O₃H⁺(m/z 131.1 ; 1 - 2 %); C₁₀H₁₆O₃H⁺(m/z 185.2 ; <
282 1%) and 4 unidentified (m/z 141.1, 155.2, 167.0 and 183.1; each < 1%).

283 The yields of formaldehyde (3 - 6 %) are in accordance with those reported by Lee et al.
284 (2006) (4 ± 2 %) who studied the reaction of α -terpinene with ozone. Moreover, the sum of
285 the yields of glyoxal and acetone (4 - 9 %) agrees with that of acetone (11%) obtained by
286 Reissell et al. (1999) for the ozonolysis reaction of γ -terpinene.

287 The sum of the yields of the 12 oxidation products identified in the gas-phase leads to a mean
288 value of \approx 50 %, which suggest that about half of the reacted γ -terpinene is not detected by the
289 PTR-MS. The missing products can be present in the gas phase but not measured by the PTR-
290 MS (multifunctional organic compounds), be lost in the inlet PEEK tubing or on the chamber
291 walls and/or partitioned to the condensed phase.

292

293 **Mechanism**

294 Several previous works (Atkinson, 1997; Calvert and Madronich, 1987; Herrmann et al.,
295 2010, Lee et al., 2006; Leungsakul et al., 2005, Mackenzie-Rae et al., 2017, Zhang and
296 Zhang, 2005) have been performed to study the gas phase reaction of monoterpenes with
297 ozone. However, to our knowledge there are no literature data describing the oxidation

298 products and the chemical mechanism related to the ozonolysis of γ -terpinene. γ -terpinene
299 contains two endocyclic C=C double bonds so, mechanistic details were evolved from
300 experimental findings and literature data of monoterpenes having one or two endocyclic
301 double bonds. Research works that have investigated the ozone reaction of α -phellandrene
302 (Mackenzie-Rae et al., 2017), limonene (Leungsakul et al., 2005), α -pinene (Zhang and
303 Zhang, 2005) and α -terpinene (Herrmann et al., 2010) were useful guides for this study. As
304 there are similarities between the chemical structure of γ -terpinene and these monoterpenes,
305 comparable degradation pathways following the ozone oxidation can be expected.

306 The reaction mechanism of γ -terpinene with ozone leading to the products listed in table 2 is
307 proposed in Figs. 5 and 6 and Figs. S3-S5. As shown in Fig. 5, the ozonolysis reaction is
308 initiated by the addition of ozone on both endocyclic C=C double bonds resulting in the
309 formation of two primary ozonides POZ1 and POZ2. The rapid decomposition of both POZs
310 through homolytic cleavage of the C–C and O–O bonds leads to the formation of four Criegee
311 intermediates (CIs) named CI1, CI2, CI3 and CI4 (Johnson and Marston, 2008). The detailed
312 degradation mechanism of CI1 is displayed in Fig. 6. Comparable schematics for CI2, CI3
313 and CI4 are provided in the Supporting Information (Figs. S3-S5), they lead to similar
314 products as those formed from CI1.

315 The CIs contain excess of energy so they are either stabilized or decompose. Stabilization of
316 CIs is achieved through unimolecular or bimolecular reactions with available atmospheric
317 species and their decomposition is believed to occur via several reaction channels (Finlayson-
318 Pitts and Pitts Jr, 1999) including the “hydroperoxide” channel (HP) which is responsible for
319 the OH formation and the “ester” channel, leading to the formation of an ester that can further
320 decompose into different compounds.

321 Hydroperoxide channel is an important pathway for CIs decomposition and it generally
322 explains the OH formation during alkene ozonolysis. Through this degradation pathway, CI1

323 rearranges into vinyl hydroperoxide before it loses an OH and decomposes into a vinyloxy
324 radical. The latter is followed by addition of oxygen molecule to form peroxy radicals. These
325 radicals further react with other peroxy radicals to form dicarbonyl compounds such as α -
326 hydroxycarbonyls having the chemical formula $C_{10}H_{16}O_3$ (m/z 185.2). A set of isomeric
327 species having the same molecular formula (same m/z value) are also suggested from the
328 different reactive channels.

329 CII may also decompose through an ester channel to form dioxirane intermediate. The
330 dissociation of the O–O bond of the dioxirane leads to the formation of diradical that
331 rearranges to form two unsaturated esters. These esters can further react with ozone to form a
332 variety of oxygenated compounds with short carbon chain.

333 In the proposed mechanism for CII, an unsaturated keto-aldehyde of chemical formula
334 $C_{10}H_{16}O_2$ (detected at $m/z = 169.2$ with the PTR-MS) probably known as γ -terpinonaldehyde
335 analogous to pinonaldehyde from α -pinene or limonaldehyde from limonene may be formed
336 from the oxygen-atom elimination channel. However as this unsaturated compound was
337 detected at low concentration by the PTR-ToF-MS (< 0.5 ppbv) one can assume that it was
338 decomposed through its reaction with ozone, may be lost on the inlet PEEK tubing of the
339 PTR-ToF-MS or on the walls of the chamber and/or partition to the particle phase rather than
340 stay in the gas phase.

341

342 **4. Conclusion and atmospheric implications**

343 Research works to study the gas-phase reaction of ozone with γ -terpinene, an important
344 monoterpene containing two endo-cyclic double bond, have been carried out in atmospheric
345 simulation chambers. The kinetic investigations and the mechanistic studies have been
346 performed for the first time at 294 ± 2 K, atmospheric pressure and under dry conditions (RH
347 < 2 %) and in the presence of cyclohexane as an OH scavenger. Two different methods, the

348 pseudo-first-order and the relative-rate method were used to determine the kinetic rate
349 coefficient for the reaction between ozone and γ -terpinene. The values obtained with both
350 methods are in good agreement and lead to a rate coefficient of $(2.10 \pm 0.11) \times 10^{-16} \text{ cm}^3$
351 molecule s^{-1} for the ozonolysis reaction of γ -terpinene. This average rate coefficient is also in
352 accordance (within the uncertainties) with that determined by Atkinson et al. (1990) using the
353 relative-rate method.

354 The oxidation products formed in the gas-phase were analyzed with a PTR-TOF-MS. 18
355 oxidation products were observed out of which 12 were identified and quantified. The molar
356 yields determined for the most abundant ones are (in %): formic acid (7 - 11), glyoxal and/or
357 acetone (4 - 9), 3-oxobutanal (6 - 8), 4-methyl-3-oxopentanal (5 - 8), acetic acid (5 - 9),
358 acetaldehyde (3 - 6), formaldehyde (3 - 6), 3-oxopropanoic acid (2 - 4) and an unidentified
359 compound with m/z 73.0 (2 - 3).

360 The rate coefficient determined in this study for the gas-phase ozonolysis of γ -terpinene
361 allows the calculation of the atmospheric lifetimes of γ -terpinene with respect to its reaction
362 with ozone. Assuming a 24-h average concentration of ozone of 100 ppbv (2.46×10^{12}
363 molecule.cm^{-3}) for a polluted area (Lin et al., 2001), the estimated lifetime of γ -terpinene in
364 the atmosphere is 32 min (see table 3). The rate coefficients of γ -terpinene with hydroxyl
365 radical and nitrate radical (IUPAC, recommended values) were previously measured and the
366 corresponding calculated lifetimes are also provided in table 3 for comparison. The reaction
367 of γ -terpinene with OH and NO_3 leads to atmospheric lifetimes of about 49 min and 2 min,
368 respectively, so the ozonolysis is also an important sink of this monoterpene in polluted areas.

369 The mechanism proposed in this study can be integrated into atmospheric models such as the
370 Master Chemical Mechanism (Saunders et al., 2003) to describe the chemistry of γ -terpinene
371 and similar endocyclic monoterpenes. Future works on the reactivity of γ -terpinene with
372 ozone should also include the identification and quantification of oxidation products formed in

373 the particle phase (secondary organic aerosol formation) under various atmospheric
374 conditions.

375

376 **Acknowledgements**

377 This work was supported by the CaPPA project (Chemical and Physical Properties of the
378 Atmosphere) funded by the French National Research Agency (ANR-11-LABX-0005-01) and
379 the CLIMIBIO program supported by the Hauts-de-France Regional Council, the French
380 Ministry of Higher Education and Research and the European Regional Development Fund.
381 The PhD grant of Layal Fayad was funded by ULCO (Université du Littoral - Côte d'Opale)
382 and PMCO (Pôle Métropolitain Côte d'Opale).

383

384 **References**

385 Atkinson, R., 1997. Gas-Phase Tropospheric Chemistry of Volatile Organic
386 Compounds: 1. Alkanes and Alkenes. *J. Phys. Chem. Ref. Data* 26, 215–290.
387 <https://doi.org/10.1063/1.556012>

388 Atkinson, R., Arey, J., 2003. Gas-phase tropospheric chemistry of biogenic volatile
389 organic compounds: a review. *Atmos. Environ.* 37, 197–219.

390 Atkinson, R., Hasegawa, D., Aschmann, S.M., 1990. Rate constants for the gas-phase
391 reactions of O₃ with a series of monoterpenes and related compounds at 296K±2 K. *Int. J.*
392 *Chem. Kinet.* 22, 871–887.

393 Avzianova, E.V., Ariya, P.A., 2002. Temperature-dependent kinetic study for
394 ozonolysis of selected tropospheric alkenes. *Int. J. Chem. Kinet.* 34, 678–684.
395 <https://doi.org/10.1002/kin.10093>

396 Blake, R.S., Monks, P.S., Ellis, A.M., 2009. Proton-Transfer Reaction Mass Spectrometry.
397 *Chem. Rev.* 109, 861-896. <https://doi.org/10.1021/cr800364q>

398 Bouvier-Brown, N.C., Goldstein, A.H., Gilman, J.B., Kuster, W.C., de Gouw, J.A., 2009. In-
399 situ ambient quantification of monoterpenes, sesquiterpenes, and related oxygenated
400 compounds during BEARPEX 2007: implications for gas- and particle-phase
401 chemistry. *Atmos. Chem. Phys.* 14, 5505-5518.

402 Calfapietra, C., Fares, S., Manes, F., Morani, A., Sgrigna, G., Loreto, F., 2013. Role of
403 Biogenic Volatile Organic Compounds (BVOC) emitted by urban trees on ozone
404 concentration
405 in cities: A review. *Environ. Pollut.* 183, 71–80.
406 <https://doi.org/10.1016/j.envpol.2013.03.012>

407 Calvert, J.G., Madronich, S., 1987. Theoretical study of the initial products of the
408 atmospheric oxidation of hydrocarbons. *J. Geophys. Res.* 92, 2211.
409 <https://doi.org/10.1029/JD092iD02p02211>

410 Finlayson-Pitts, B.J., Pitts Jr, J.N., 1999. Chemistry of the upper and lower
411 atmosphere: theory, experiments, and applications. Academic Press.

412 Guenther, A., Hewitt, C.N., Erickson, D., Fall, R., Geron, C., Graedel, T., Harley, P.,
413 Klinger, L., Lerdau, M., Mckay, W.A., Pierce, T., Scholes, B., Steinbrecher, R., Tallamraju,
414 R., Taylor, J., Zimmerman, P., 1995. A global model of natural volatile organic compound
415 emissions. *J. Geophys. Res.* 100, 8873. <https://doi.org/10.1029/94JD02950>

416 Grimsrud E.P, Westberg H.H, Rasmussen R.A, 1975. Atmospheric reactivity of
417 monoterpene hydrocarbons, NO_x photooxidation and ozonolysis. *Int. J. Chem. Kinet.*, 7(1):
418 183-195.

419 Henry, K.M., Donahue, N.M., 2011. Effect of the OH Radical Scavenger Hydrogen
420 Peroxide on Secondary Organic Aerosol Formation from α -Pinene Ozonolysis. *Aerosol Sci.*
421 *Technol.* 45, 696–700. <https://doi.org/10.1080/02786826.2011.552926>

422 Herrmann, F., Winterhalter, R., Moortgat, G.K., Williams, J., 2010. Hydroxyl radical
423 (OH) yields from the ozonolysis of both double bonds for five monoterpenes. *Atmos.*
424 *Environ.* 44, 3458–3464. <https://doi.org/10.1016/j.atmosenv.2010.05.011>

425 Hoffmann, T., Odum, J.R., Bowman, F., Collins, D., Klockow, D., Flagan, R.C.,
426 Seinfeld, J.H., 1997. Formation of organic aerosols from the oxidation of biogenic
427 hydrocarbons. *J. Atmospheric Chem.* 26, 189–222.

428 IUPAC. IUPAC Task Group on Atmospheric Chemical Kinetic Data Evaluation,
429 (<http://iupac.pole-ether.fr>)

430 Johnson, D., Marston, G., 2008. The gas-phase ozonolysis of unsaturated volatile
431 organic compounds in the troposphere. *Chem. Soc. Rev.* 37, 699.
432 <https://doi.org/10.1039/b704260b>

433 Keywood, M.D., Kroll, J.H., Varutbangkul, V., Bahreini, R., Flagan, R.C., Seinfeld,
434 J.H., 2004. Secondary Organic Aerosol Formation from Cyclohexene Ozonolysis: Effect of
435 OH Scavenger and the Role of Radical Chemistry. *Environ. Sci. Technol.* 38, 3343–3350.
436 <https://doi.org/10.1021/es049725j>

437 Khalil, M.A.K., Rasmussen, R.A., 1992. Forest Hydrocarbon Emissions: Relationships
438 Between Fluxes and Ambient Concentrations. *J. Air Waste Manag. Assoc.* 42, 810–813.
439 <https://doi.org/10.1080/10473289.1992.10467033>

440 Lamb, B., Guenther, A., Gay, D., Westberg, H., 1987. A national inventory of
441 biogenic hydrocarbon emissions. *Atmospheric Environ.* 1987 21, 1695–1705.
442 [https://doi.org/10.1016/0004-6981\(87\)90108-9](https://doi.org/10.1016/0004-6981(87)90108-9)

443 Lauraguais, A., Coeur-Tourneur, C., Cassez, A., Seydi, A., 2012. Rate constant and
444 secondary organic aerosol yields for the gas-phase reaction of hydroxyl radicals with syringol
445 (2,6-dimethoxyphenol). *Atmos. Environ.* 55, 43–48.
446 <https://doi.org/10.1016/j.atmosenv.2012.02.027>

447 Lee, A., Goldstein, A.H., Kroll, J.H., Ng, N.L., Varutbangkul, V., Flagan, R.C.,
448 Seinfeld, J.H., 2006. Gas-phase products and secondary aerosol yields from the
449 photooxidation of 16 different terpenes. *J. Geophys. Res.* 111.
450 <https://doi.org/10.1029/2006JD007050>

451 Leungsakul, S., Jaoui, M., Kamens, R.M., 2005. Kinetic Mechanism for Predicting
452 Secondary Organic Aerosol Formation from the Reaction of *d* -Limonene with Ozone.
453 *Environ. Sci. Technol.* 39, 9583–9594. <https://doi.org/10.1021/es0492687>

454 Lin, C.-Y. C.; Jacob, D. J.; Fiore, A. M. Trends in Exceedances of the Ozone Air
455 Quality Standard in the Continental United States, 1980–1998. *Atmos. Environ.* 2001, 35,
456 3217–3228.

457 Ma, Y., Marston, G., 2009. Formation of organic acids from the gas-phase ozonolysis
458 of terpinolene. *Phys. Chem. Chem. Phys.* 11, 4198. <https://doi.org/10.1039/b818789d>

459 Mackenzie-Rae, F.A., Liu, T., Deng, W., Saunders, S.M., Fang, Z., Zhang, Y., Wang,
460 X., 2017. Ozonolysis of α -phellandrene – Part 1: Gas- and particle-phase characterisation.
461 *Atmos. Chem. Phys.* 17, 6583–6609. <https://doi.org/10.5194/acp-17-6583-2017>

462 Martínez, E., Cabañas, B., Aranda, A., Martín, P., and Salgado, S., J. 1999 Absolute
463 Rate Coefficients for the Gas-Phase Reactions of NO₃ Radicals with a Series of Monoterpenes
464 at T=298 to 433 K. *Atmos. Chem.*, 33, 265- 282.

465 Peñuelas, J., Staudt, M., 2010. BVOCs and global change. *Trends Plant Sci.* 15, 133–
466 144. <https://doi.org/10.1016/j.tplants.2009.12.005>

467 Reissell, A., Harry, C., Aschmann, S.M., Atkinson, R., Arey, J., 1999. Formation of
468 acetone from the OH radical- and O₃-initiated reactions of a series of monoterpenes. *J.*
469 *Geophys. Res.* 104, 13869–13879.

470 Saunders, S. M., Jenkin, M. E., Derwent, R. G., and Pilling, M.J.: Protocol for the
471 development of the Master Chemical Mechanism, MCM v3 (Part A): tropospheric

472 degradation of nonaromatic volatile organic compounds, *Atmos. Chem. Phys.*, 3, 161–180,
473 <https://doi.org/10.5194/acp-3-161-2003>, 2003.

474 Smith, D., Španěl, P., 2005. Selected ion flow tube mass spectrometry (SIFT-MS) for
475 on-line trace gas analysis. *Mass Spectrom. Rev.* 24, 661–700.
476 <https://doi.org/10.1002/mas.20033>

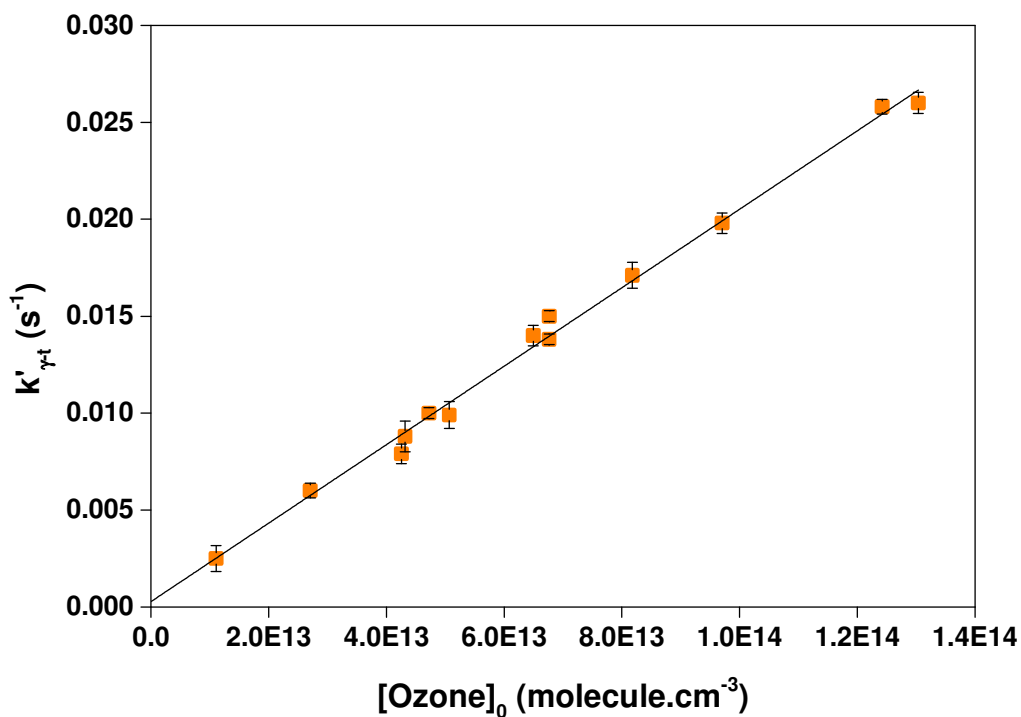
477 Wang, X., Liu, T., Bernard, F., Ding, X., Wen, S., Zhang, Y., Zhang, Z., He, Q., Lü,
478 S., Chen, J., Saunders, S., Yu, J., 2014. Design and characterization of a smog chamber for
479 studying gas-phase chemical mechanisms and aerosol formation. *Atmos. Meas. Tech.* 7, 301–
480 313. <https://doi.org/10.5194/amt-7-301-2014>

481 Witter, M., Berndt, T., Böge, O., Stratmann, F., Heintzenberg, J., 2002. Gas-phase
482 ozonolysis: Rate coefficients for a series of terpenes and rate coefficients and OH yields for 2-
483 methyl-2-butene and 2,3-dimethyl-2-butene: Gas-Phase Ozonolysis. *Int. J. Chem. Kinet.* 34,
484 394–403. <https://doi.org/10.1002/kin.10063>

485 Zhang, D., Zhang, R., 2005. Ozonolysis of α -pinene and β -pinene: Kinetics and
486 mechanism. *J. Chem Phys.* 122, 114308. <https://doi.org/10.1063/1.1862616>

1 **Fig. 1.** Plot of the pseudo-first-order rate coefficients ($k'_{\gamma t}$) for the reaction of O_3 with γ -
2 terpinene as a function of the initial ozone concentration, obtained at $294 \pm 2K$, atmospheric
3 pressure and in the presence of an ozone scavenger (cyclohexane). The error bars vary in the
4 range 0.03-0.07 % and reflect the uncertainties on the measurements of $k'_{\gamma t}$.

5

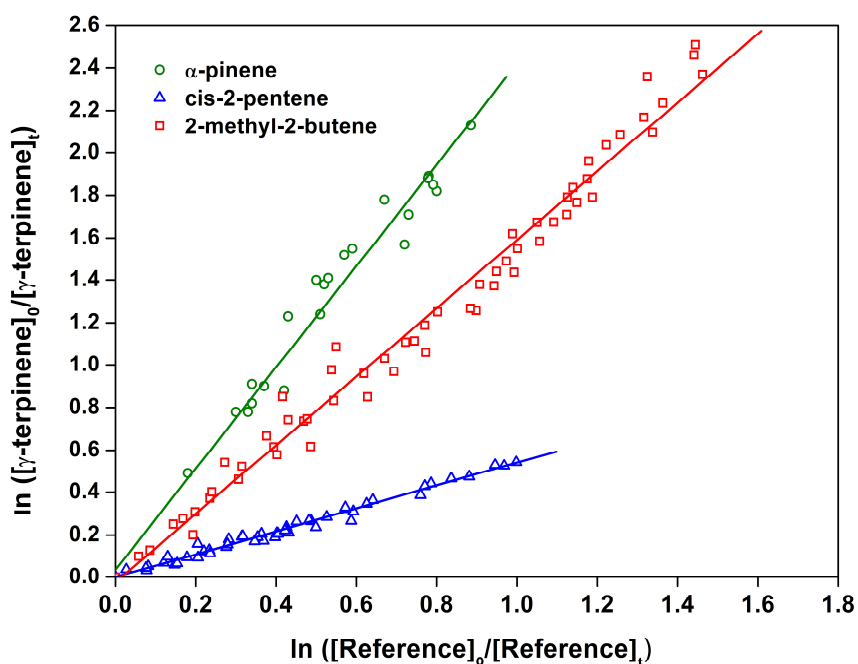


6
7

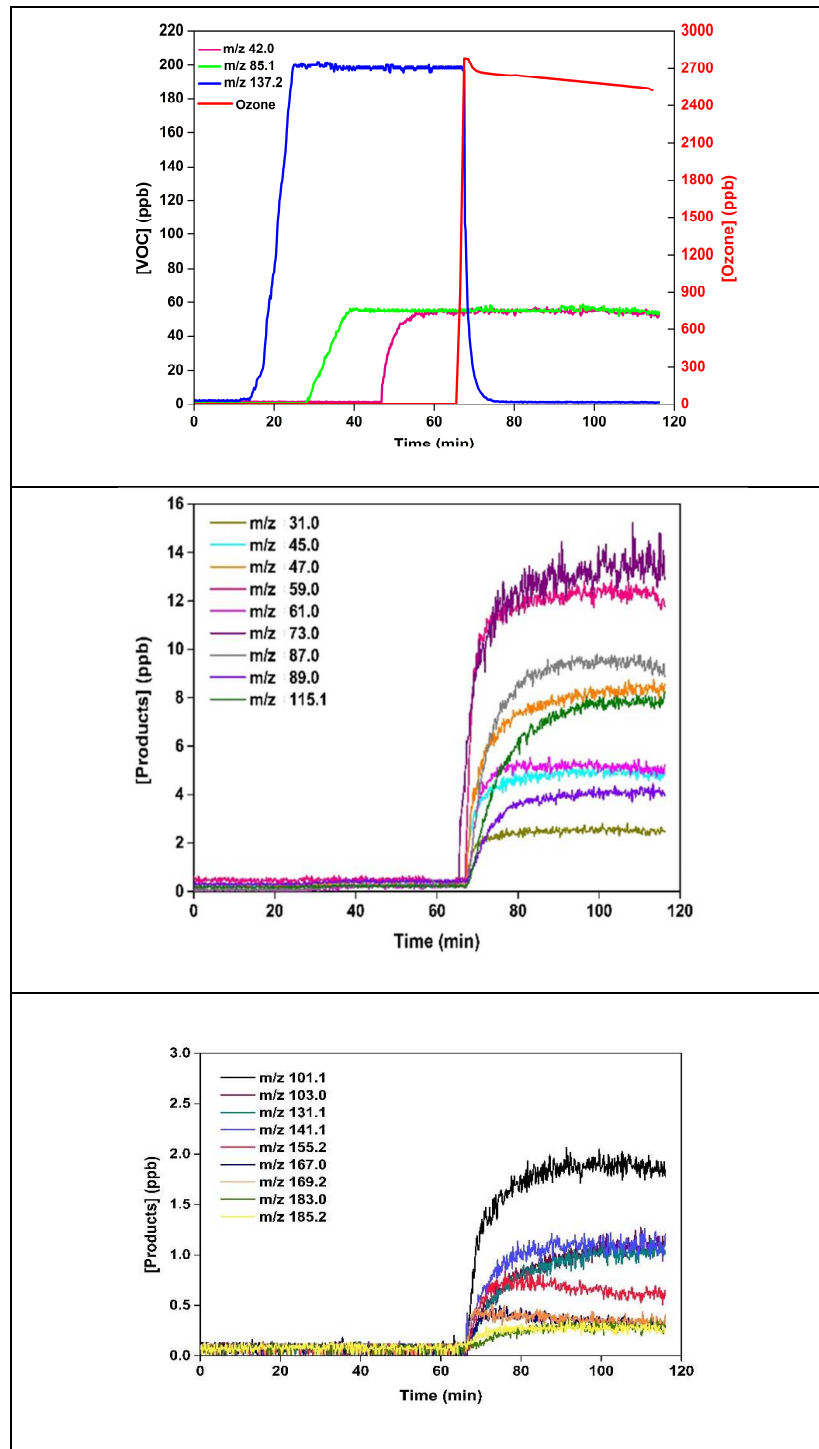
8 **Fig. 2.** Relative rate plots for the reaction of γ -terpinene with ozone obtained at $294 \pm 2\text{K}$,
9 atmospheric pressure and in the presence of an ozone scavenger (cyclohexane). Three
10 references were used: cis-2-pentene (red squares; PTR-ToF-MS analyses), 2-methyl-2-butene
11 (blue triangle; PTR-ToF-MS analyses) and α -pinene (green circles; GC-MS analyses).

12

13

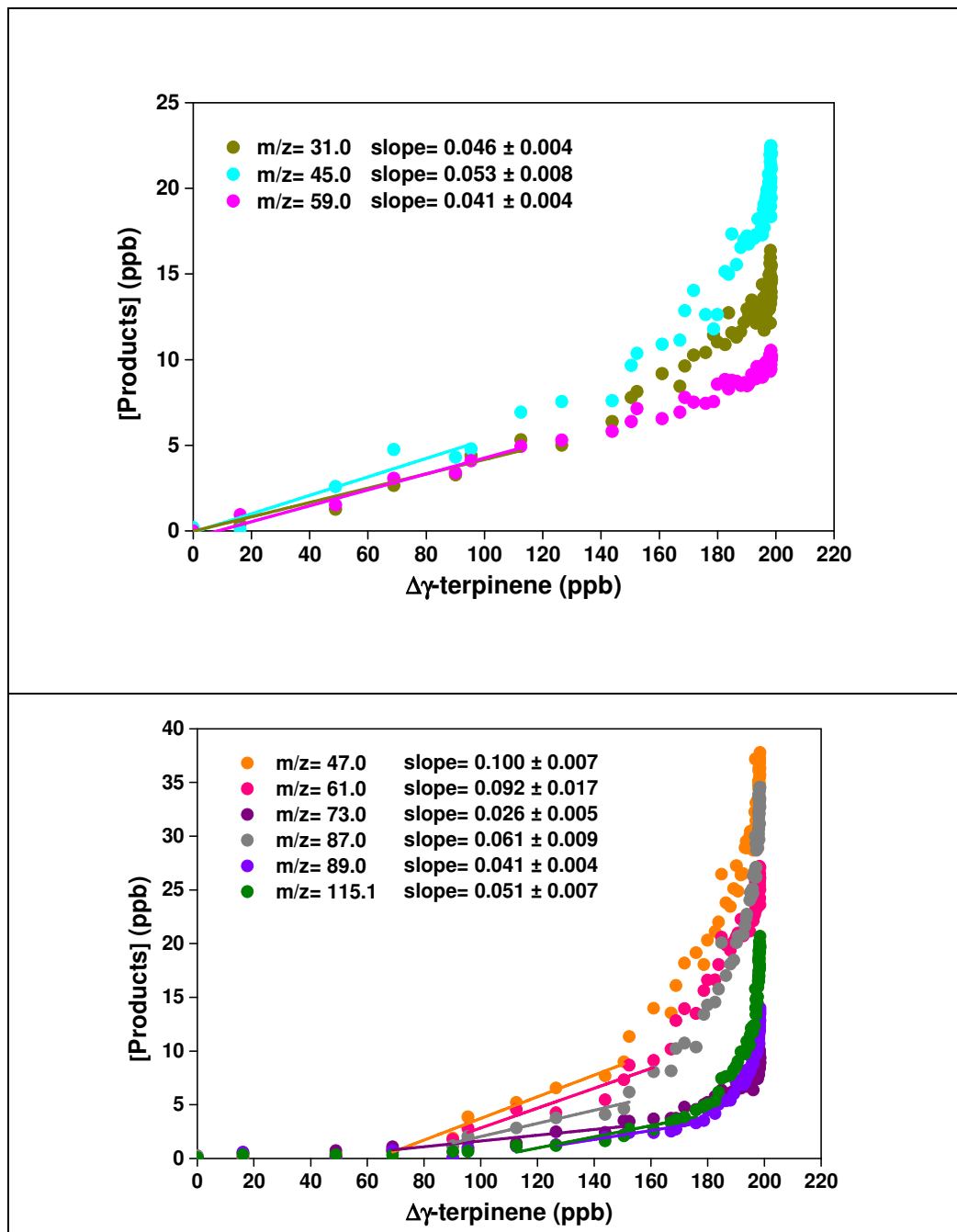


14 **Fig. 3.** Typical time profiles of chemical compounds detected by PTR-ToF-MS and ozone
 15 analyzer during the ozonolysis of γ -terpinene (initial concentrations: γ -terpinene 200 ppbv ; O₃
 16 2780 ppbv). Note that m/z includes the addition of H⁺. a) reactants (m/z): γ -terpinene (137.2),
 17 cyclohexane (ozone scavenger; 85.1) and acetonitrile (dilution tracer; 42.0); b) major oxidation
 18 products; c) minor oxidation products. The compounds corresponding to the m/z ratios are listed
 19 in table 2.



21 **Fig. 4.** Typical plot for the determination of the gas-phase product yields formed from the
22 ozonolysis of γ -terpinene (initial concentrations: γ -terpinene 200 ppbv and O_3 2780 ppbv). Note
23 that m/z includes the addition of H^+ .

24

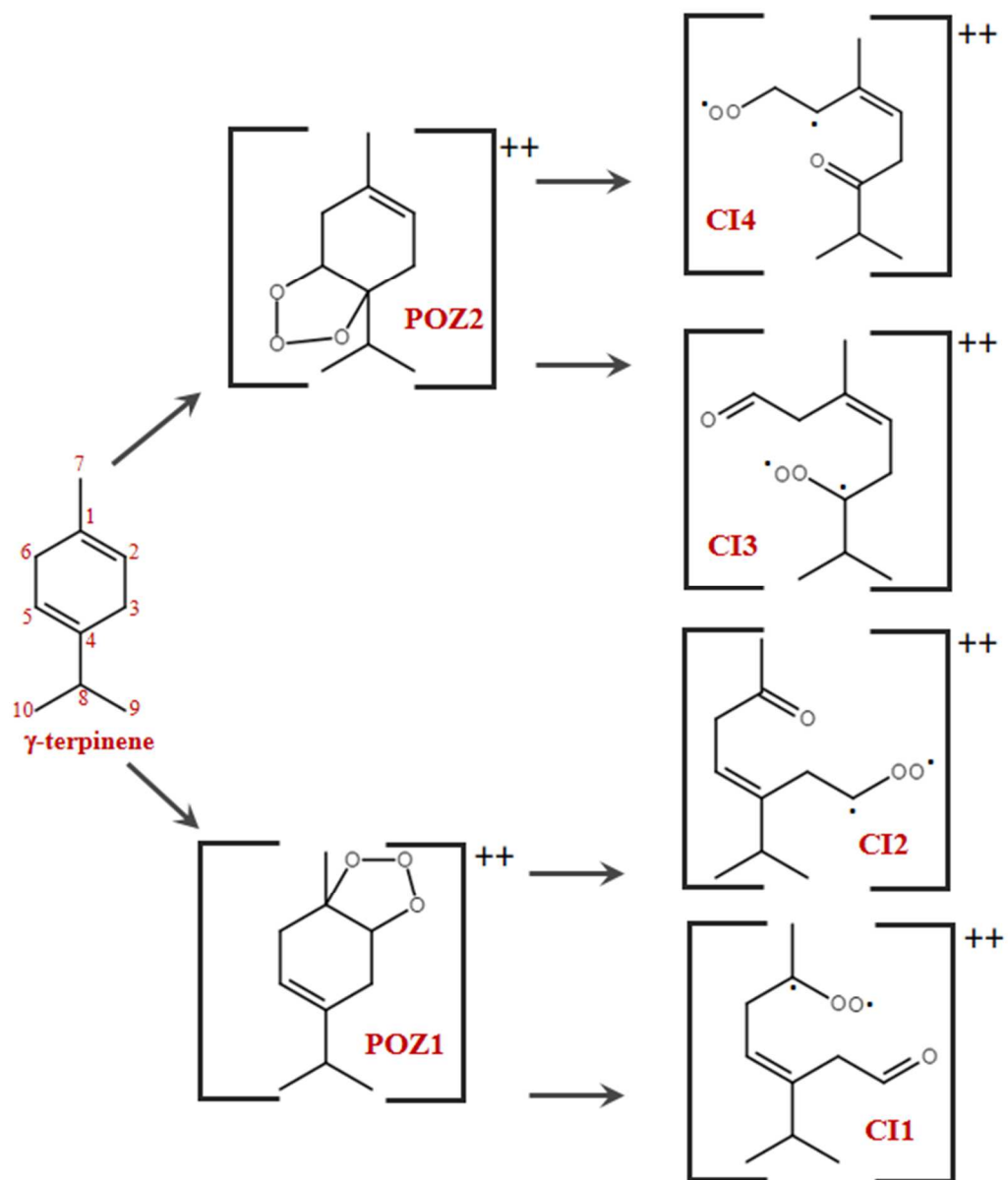


25

26

27 **Fig. 5.** Simplified mechanism for the formation of primary ozonides (POZs) and Criegee
28 intermediates (CIs) from the reaction of γ -terpinene with ozone.

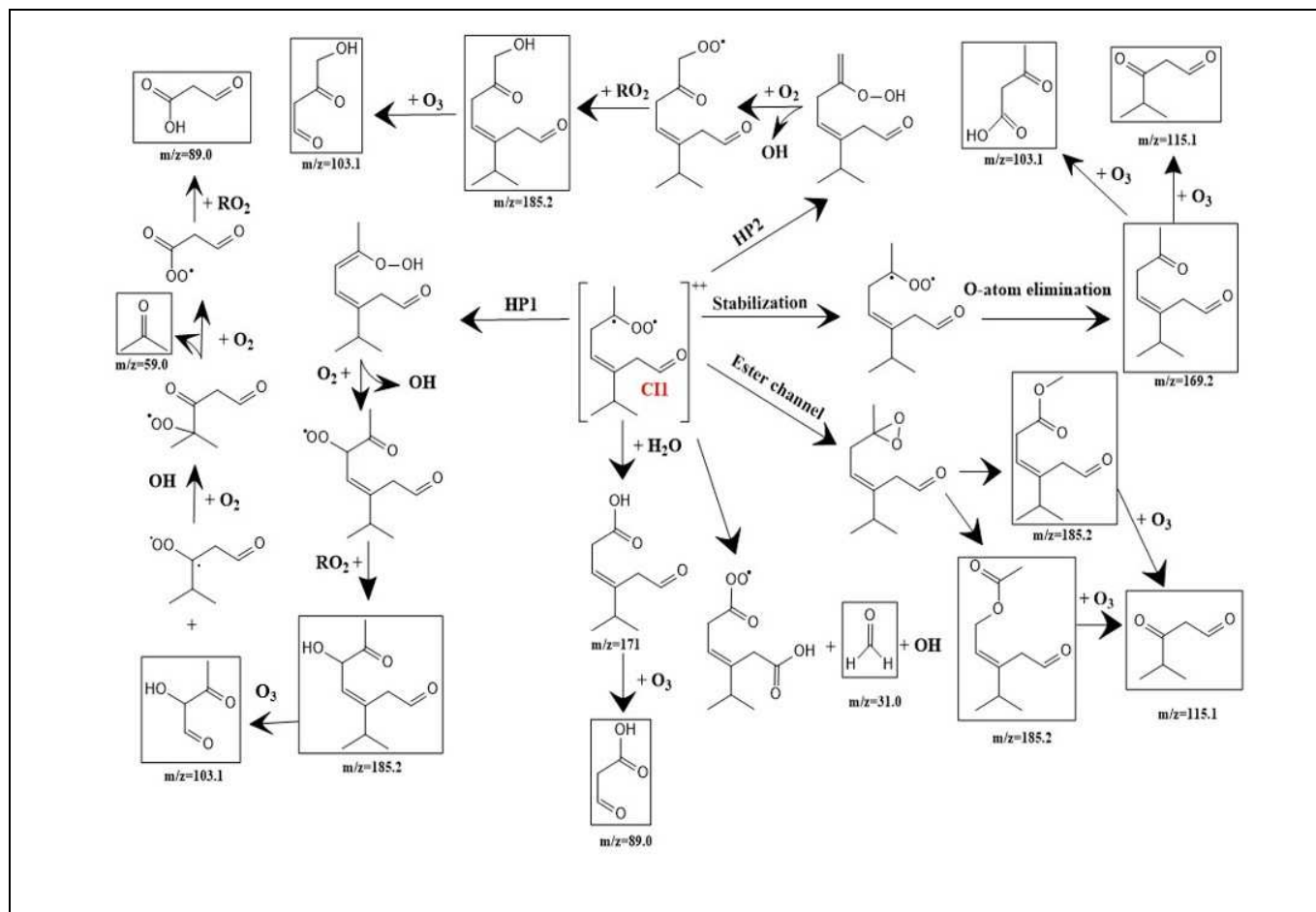
29



30
31

32 **Fig. 6.** The mechanism for the ozonolysis of γ -terpinene starting from C11, and yielding
 33 different products detected by the PTR-ToF-MS. Comparable schematics for the remaining CIs
 34 are provided in the Supporting Information (Fig. S3-S5).

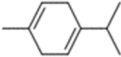
35



36

37

1 **Table 1.** Rate coefficient determined for the reaction of γ -terpinene with ozone at 294 ± 2 K,
 2 atmospheric pressure and literature data.

| Compound | Method | Reference | $k_{\gamma\text{-t}}/k_{\text{ref}}^a$ | $k_{\gamma\text{-t}}^b$ ($\times 10^{-16}$) | $k_{\gamma\text{-t}}^{b,c}$ ($\times 10^{-16}$) | $k_{\gamma\text{-t}}^{b,d}(\text{average})$ ($\times 10^{-16}$) | Literature |
|--|--------------------|------------------------------------|--|--|--|--|--------------------------|
| γ -terpinene $\text{C}_{10}\text{H}_{16}$  | Pseudo first order | - | - | 2.03 ± 0.11^h | | | |
| | Relative | 2-methyl-2-butene ^e | 0.53 ± 0.02 | 2.17 ± 0.08^a | | 2.10 ± 0.11 | This study |
| | | <i>cis</i> -2-pentene ^f | 1.61 ± 0.06 | 2.13 ± 0.13^a | 2.17 ± 0.11 | | |
| | | α -pinene ^g | 2.29 ± 0.14 | 2.23 ± 0.13^a | | | |
| | Absolute | - | - | 2.84 | - | - | (Grimsrud, et al., 1974) |
| Relative | α -pinene | - | - | 1.63 ± 0.12^i | - | - | (Atkinson et al., 1990) |

3 ^a Indicated errors are twice the standard deviation arising from the linear regression analysis and do not include the
 4 uncertainty in the reference rate coefficients.

5 ^b Expressed in $\text{cm}^3 \text{ molecule}^{-1} \text{ s}^{-1}$.

6 ^c Determined using plots based on eq V (see the text).

7 ^d Average rate coefficient for both methods.

8 ^e $k_{(2\text{-methyl-2-butene} + \text{O}_3)} = (4.1 \pm 0.5) \times 10^{-16} \text{ cm}^3 \text{ molecule}^{-1} \text{ s}^{-1}$ (Witter et al. 2002).

9 ^f $k_{(\text{cis-2-pentene} + \text{O}_3)} = (1.32 \pm 0.04) \times 10^{-16} \text{ cm}^3 \text{ molecule}^{-1} \text{ s}^{-1}$ (Avzianova and Ariya 2002).

10 ^g $k_{(\alpha\text{-pinene} + \text{O}_3)} = (9.6 \pm 0.15) \times 10^{-17} \text{ cm}^3 \text{ molecule}^{-1} \text{ s}^{-1}$ at 298 K (IUPAC, recommended value).

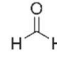
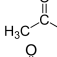
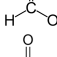
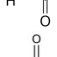
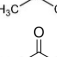
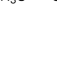
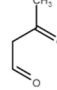
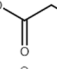
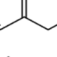
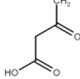
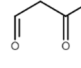
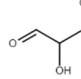
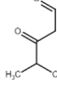
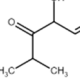
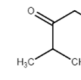
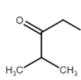
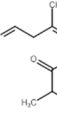
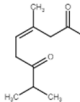
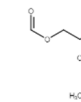
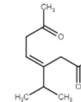
11 ^h Indicated errors include both the relative uncertainties on the determination of $k_{\gamma\text{-t}}^b$ (twice the standard deviation
 12 arising from the linear regression analysis) and that on the measurement of the O_3 concentration (relative
 13 uncertainty = 5%).

14 ⁱ Recalculated using the current recommended value (IUPAC) for the α -pinene rate coefficient.

15

16

17 **Table 2.** Ions detected by the PTR-ToF-MS during the gas-phase reaction of γ -terpinene with
 18 ozone (m/z masses include the addition of H^+). Identification of the oxidation products and
 19 formation yields (the indicated ranges correspond to the values obtained from all experiments).

| m/z | Formula | Name | Structure | Yield range (%) |
|-------|----------------------|----------------------------|---|-----------------|
| 31.0 | CH_2OH^+ | Formaldehyde |  | 3 - 6 |
| 45.0 | $C_2H_4OH^+$ | Acetaldehyde |  | 3 - 6 |
| 47.0 | $CH_2O_2H^+$ | Formic acid |  | 7 - 11 |
| 59.0 | $C_2H_2O_2H^+$ | Glyoxal |  | 4 - 9 |
| | $C_3H_6OH^+$ | Acetone |  | |
| 61.0 | $C_2H_4O_2H^+$ | Acetic acid |  | 5 - 9 |
| 73.0 | $C_3H_4O_2H^+$ | Unidentified | | 2 - 3 |
| 87.0 | $C_4H_6O_2H^+$ | 3-oxobutanal |  | 6 - 8 |
| 89.0 | $C_3H_4O_3H^+$ | 3-oxopropanoic acid |  | 2 - 4 |
| 101.0 | $C_4H_4O_3H^+$ | 2-Oxosuccinaldehyde |  | < 1 |
| 103.1 | $C_4H_6O_3H^+$ | - |    | 1 - 2 |
| 115.1 | $C_6H_{10}O_2H^+$ | 4-methyl-3-oxo-pentanal |  | 5 - 8 |
| 131.1 | $C_6H_{10}O_3H^+$ | - |    | 1 - 2 |
| 141.1 | Unidentified | - | | < 1 |
| 155.2 | Unidentified | - | | < 1 |
| 167.0 | Unidentified | - | | < 1 |
| 169.2 | $C_{10}H_{16}O_2H^+$ | γ -terpinonaldehyde |  | < 1 |
| 183.0 | Unidentified | - | | < 1 |
| 185.2 | $C_{10}H_{16}O_3H^+$ | - |    | < 1 |

20

21

22 Table 3: Atmospheric life-time of γ -terpinene with different oxidants.

| $\tau(\text{OH})^{\text{a}}$ | $\tau(\text{NO}_3)^{\text{b}}$ | $\tau(\text{O}_3)^{\text{c}}$ |
|------------------------------|--------------------------------|-------------------------------|
| 49 min | 2 min | 32 min |

- 23
- 24 ^aAssumed OH radical concentration: 2.0×10^6 molecules. cm^{-3} , 12-h daytime average (Atkinson and Arey, 2003)
- 25 and calculated with $k_{(\gamma\text{-terpinene} + \text{OH})} = 1.7 \times 10^{-10}$ $\text{cm}^3 \cdot \text{molecule}^{-1} \cdot \text{s}^{-1}$ (IUPAC recommended value).
- 26 ^bAssumed NO_3 radical concentration: 2.5×10^8 molecules. cm^{-3} , 12-h nighttime average (Atkinson and Arey, 2003)
- 27 and calculated with $k_{(\gamma\text{-terpinene} + \text{NO}_3)} = 2.9 \times 10^{-11}$ $\text{cm}^3 \cdot \text{molecule}^{-1} \cdot \text{s}^{-1}$ (IUPAC recommended value).
- 28 ^cAssumed O_3 concentration: 2.46×10^{12} molecules. cm^{-3} (100 ppbv), polluted atmosphere (Lin et al., 2001) and
- 29 calculated with $k_{(\gamma\text{-terpinene} + \text{O}_3)} = (2.10 \pm 0.11) \times 10^{-16}$ $\text{cm}^3 \cdot \text{molecule}^{-1} \cdot \text{s}^{-1}$ (this study).